Maximum Urban Heat Island Intensity in Seoul

YEON-HEE KIM* AND JONG-JIN BAIK+

Department of Environmental Science and Engineering, Kwangju Institute of Science and Technology, Kwangju, Korea

(Manuscript received 5 March 2001, in final form 10 December 2001)

ABSTRACT

The maximum urban heat island (UHI) intensity in Seoul, Korea, is investigated using data measured at two meteorological observatories (an urban site and a rural site) during the period of 1973–96. The average maximum UHI is weakest in summer and is strong in autumn and winter. Similar to previous studies for other cities, the maximum UHI intensity is more frequently observed in the nighttime than in the daytime, decreases with increasing wind speed, and is pronounced for clear skies. A multiple linear regression analysis is performed to relate the maximum UHI to meteorological elements. Four predictors considered in this study are the maximum UHI intensity for the previous day, wind speed, cloudiness, and relative humidity. The previous-day maximum UHI intensity is positively correlated with the maximum UHI, and the wind speed, cloudiness, and relative humidity are negatively correlated with the maximum UHI intensity. Among the four predictors, the previous-day maximum UHI intensity is the most important. The relative importance among the predictors varies depending on time of day and season. A three-layer back-propagation neural network model with the four predictors as input units is constructed to predict the maximum UHI intensity in Seoul, and its performance is compared with that of a multiple linear regression model. For all test datasets, the neural network model improves upon the regression model in predicting the maximum UHI intensity. The improvement of the neural network model upon the regression model is 6.3% for the unstratified test data, is higher in the daytime (6.1%) than in the nighttime (3.3%), and ranges from 0.8% in spring to 6.5% in winter.

1. Introduction

In most big cities, urbanization has produced significant changes in the surface and atmospheric properties that can subsequently result in inadvertent local weather and climate changes (Changnon 1981; Cotton and Pielke 1995). The urban heat island (UHI) phenomenon, in which surface air temperature in an urban area is higher than in the surrounding suburbs and rural area, is a feature commonly observed in many cities, and its characteristics have been extensively studied during the past several decades (Oke 1987). Urban-induced or -modified weather and climate changes have received much attention. Among these, urban effects on precipitation have been of particular scientific interest (Lowry 1998). There are some theoretical (Lin and Smith 1986; Baik and Chun 1997) and numerical (Baik et al. 2001) studies investigating convection and precipitation forced by UHIs.

The UHI intensity is closely linked to local meteorological conditions. It is well known that UHIs are prominent at clear and windless night (e.g., Yague et al. 1991; Klysik and Fortuniak 1999; Montavez et al. 2000). The UHI intensity can exhibit diurnal and seasonal cycles and is modulated by cloud and wind conditions (Ackerman 1985). Yague et al. (1991) showed that the maximum UHI intensity in Madrid, Spain, is observed in anticyclonic weather events (corresponding to clear skies) during cold periods. Anthropogenically generated heat also affects UHI intensity, with its impact being especially strong in winter (Oke et al. 1991).

Sundborg (1950) was the first to relate UHI intensity to meteorological elements such as cloudiness, wind speed, temperature, and absolute humidity using a multiple linear regression method. He showed that cloudiness and wind speed parameters are negatively correlated with the UHI intensity in Uppsala, Sweden, and that the total variance explained by the regression model is larger in the nighttime than in the daytime. After Sundborg's pioneering paper was published, many similar works have followed, using different sets of meteorological parameters for various cities (e.g., Duckworth and Sandberg 1954; Morris et al. 2001).

An artificial neural network, or simply a neural network, can be an alternative method to a standard regression method. Because a neural network can handle

* Current affiliation: Meteorological Research Institute, Seoul, Korea.

+ Current affiliation: Seoul National University, Seoul, Korea.

Corresponding author address: Jong-Jin Baik, School of Earth and Environmental Sciences, Seoul National University, Seoul 151-742, Korea.
E-mail: jjbaik@snu.ac.kr

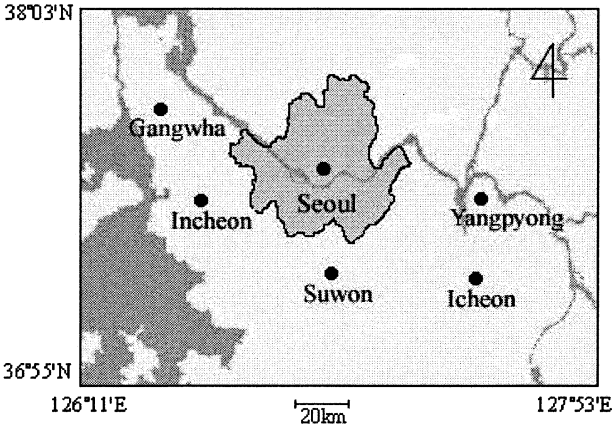

FIG. 1. The locations of meteorological observatories selected for this study. Seoul observatory (37°34′N, 126°58′E) is located at an altitude of 86 m above the mean sea level, Yangpyong observatory (37°29′N, 127°30′E) at an altitude of 49 m. The distance between Seoul and Yangpyong observatories is 60 km. The boundary between Seoul and its surroundings is drawn with a solid line.

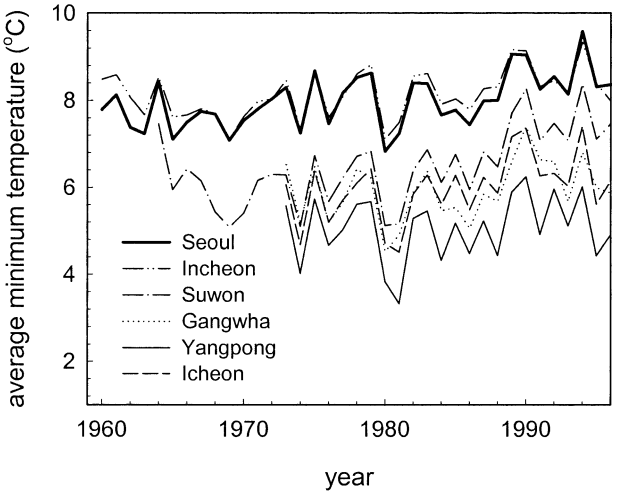

FIG. 2. The time series of annually averaged minimum temperature at Seoul, Incheon, Suwon, Gangwha, Yangpyong, and Icheon observatories.

unknown nonlinear behavior well, it has been successfully adopted in solving relevant problems in meteorology and oceanography (Hsieh and Tang 1998). Santamouris et al. (1999) modeled the distribution of surface air temperature in Athens, Greece, during summer seasons with a neural network approach and were successful in predicting air temperature. They used, however, only temperature as input data.

This study is concerned with the maximum UHI intensity and its prediction in Seoul, Korea, and is undertaken with two specific objectives. The first objective is to characterize the maximum UHI intensity in Seoul and relate it to meteorological elements using a multiple linear regression method. The second objective is to develop a neural network model for the prediction of the maximum Seoul UHI intensity and demonstrate the potential of the neural network model in predicting UHI intensity by comparing its performance with that of the multiple linear regression model. For this study, 24 years of data collected at two meteorological observatories, representing an urban site and a rural site, are used.

2. Site selection and data description

The data used in this study are from archives of the Korea Meteorological Administration and consist of surface observations at Seoul and its nearby meteorological observatories (Fig. 1). Seoul is the capital of, and the largest city in, Korea. Seoul, which is located in the central western part of the Korean peninsula, has a population of about 10 million people. The Seoul observatory is located in the central region of Seoul and surrounded by dense low-rise buildings. The sky view factor at the measurement location is large because the location of the observatory is slightly elevated topographically. Incheon, located west of Seoul, is one of the six largest cities in Korea. Suwon, located south of Seoul, has been urbanized rapidly during the past 20 years, as evidenced by a rapid increase in minimum temperature (Fig. 2). Gangwha, Yangpyong, and Icheon are located in the suburbs and rural areas of Seoul. Climate in Korea is temperate, with distinct daily and seasonal temperature variations and with maximum precipitation being concentrated in the summer.

Figure 2 shows the time series of annually averaged minimum temperature at the six observatories. All of the time series exhibit an increasing trend since about 1980 and similar year-to-year fluctuation patterns. A study of UHI intensity conventionally requires an elimination of the effects of large-scale changes and hence an isolation of local effects. A technique most commonly used to detect the influence of urbanization is to consider a difference in temperature between representative urban and rural stations (Yague et al. 1991; Jauregui et al. 1992; Karaca et al. 1995). The latitude and elevation of Seoul observatory (37°34′N and 86 m) are very similar to those of Yangpyong observatory (37°29′N and 49 m), and the largest temperature difference between Seoul and any rural observatories is observed when Yangpyong is selected (Fig. 2). Gangwha observatory is very close to the sea (Yellow Sea) and Icheon observatory is located farther southeast of Seoul (Fig. 1). Considering these facts, Yangpyong appears to be the best choice as the representative rural site among the three suburbs and rural observatories. In this study, the daily maximum Seoul UHI intensity is defined as the maximum temperature difference between Seoul and Yangpyong.

The data used for investigating the maximum UHI intensity in Seoul span the years from 1973 to 1996. Continuous surface observations have been made at Yangpyong observatory since 1973. The data utilized for analysis consist of observations of surface air tem-

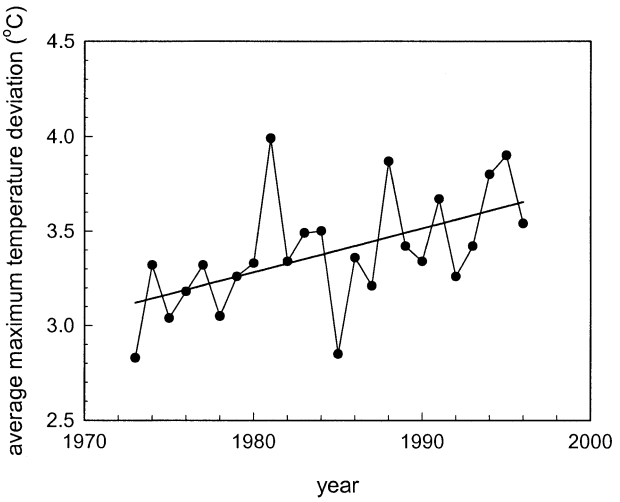

FIG. 3. The time series of annually averaged maximum temperature deviation between Seoul and Yangpyong observatories. The linear regression line is drawn.

perature at Seoul and Yangpyong observatories and of wind speed, cloudiness, and relative humidity at Seoul observatory, all in 6-h intervals. Cloudiness is expressed as values of 0–10, where 0 indicates no clouds and 10 indicates overcast skies. The value of cloudiness is assigned as 10 when it is rainy or snowy or foggy. The sample size for each meteorological element is 8765 observations during the 24-yr period. The maximum UHI intensity is negative (when the temperature at Yangpyong observatory is higher than that at Seoul observatory) for 4% of the total data.

3. Analysis of the maximum UHI intensity in Seoul

a. Characteristics of the maximum UHI intensity

Figure 3 shows the time series of annually averaged maximum UHI intensity in Seoul. The average UHI intensity exhibits a gradual increase trend with time (0.56°C over 24 years, from the linear regression line) and some year-to-year variations. Figure 4 shows the time series of seasonally averaged maximum UHI in-

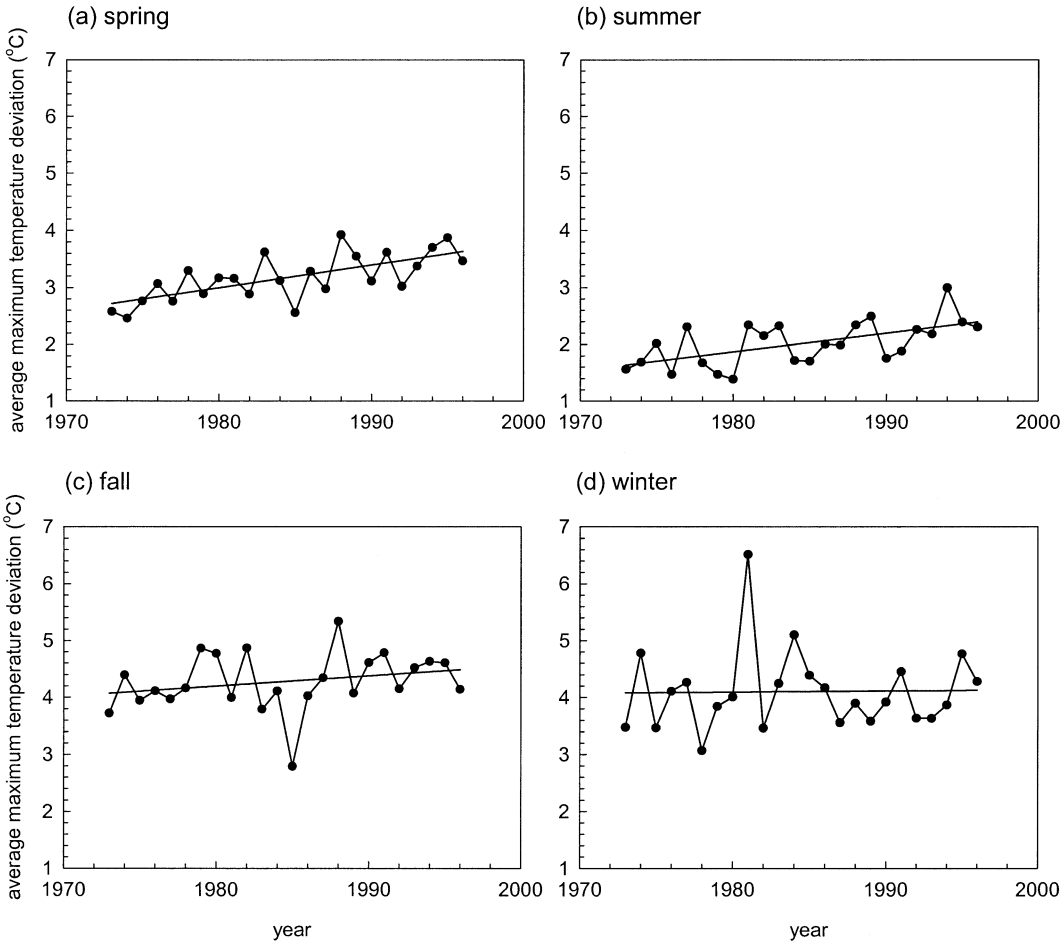

FIG. 4. The time series of seasonally averaged maximum temperature deviation between Seoul and Yangpyong observatories. The linear regression line for each season is drawn.

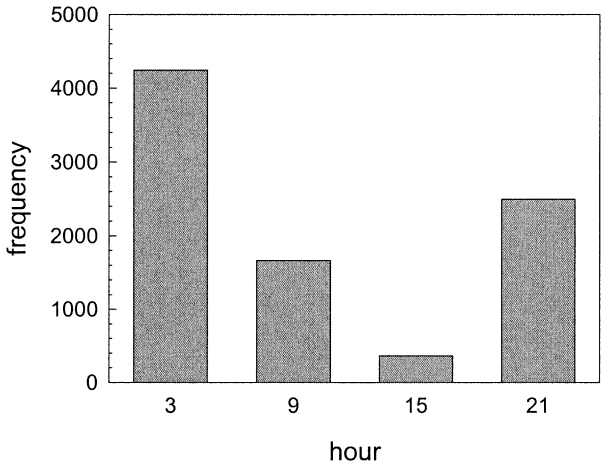

FIG. 5. The histogram of the frequency distribution of the maximum temperature deviation between Seoul and Yangpyong observatories as a function of time of day.

tensity. The average maximum UHI intensity is weakest in summer and strong in autumn and winter. Autumn and winter in Seoul are drier than summer, which is commensurate with Jauregui et al.'s (1992) result that the UHI intensity in Mexico City, Mexico, is largest during the dry season. Over the 24-yr period, the maximum average UHI intensity most rapidly increased with time for spring (0.95°C over 24 years, from the linear regression line). On the other hand, for winter, the maximum UHI intensity has no significant trend. Figure 5 shows the histogram of the frequency distribution of the maximum UHI as a function of time of day. The maximum UHI is more frequently observed in the nighttime (2100 and 0300 local standard time) than in the daytime (0900 and 1500 local standard time). This fact is due to nocturnal radiative cooling in the rural area and the effects of a large heat capacity in the urban area. The frequency of the maximum in the nighttime is 3.3 times larger than in the daytime.

Many previous studies indicated that the UHI intensity is strong during clear and windless nights (e.g., Montavez et al. 2000). To investigate the effect of each meteorological parameter on the Seoul UHI intensity, the frequency distribution of the maximum UHI intensity as a function of wind speed, relative humidity, and cloudiness is plotted in Fig. 6. For wind speeds greater than about 0.8 m s^{-1}, the maximum UHI intensity decreases as the wind speed increases (Fig. 6a). For very strong winds, the thermal contrast between the two sites disappears. This behavior suggests that there can be a critical wind speed beyond which the UHI phenomenon is not noticeable. If the cases with the maximum UHI intensity being less than 0.3°C are considered as indicative of the absence of UHI, the critical wind speed is approximately 7.0 m s^{-1}. In the relative humidity plot (Fig. 6b), 72% of the total data exists in the 60%–90% relative humidity range. It is difficult from this figure to find a particular relationship between the maximum

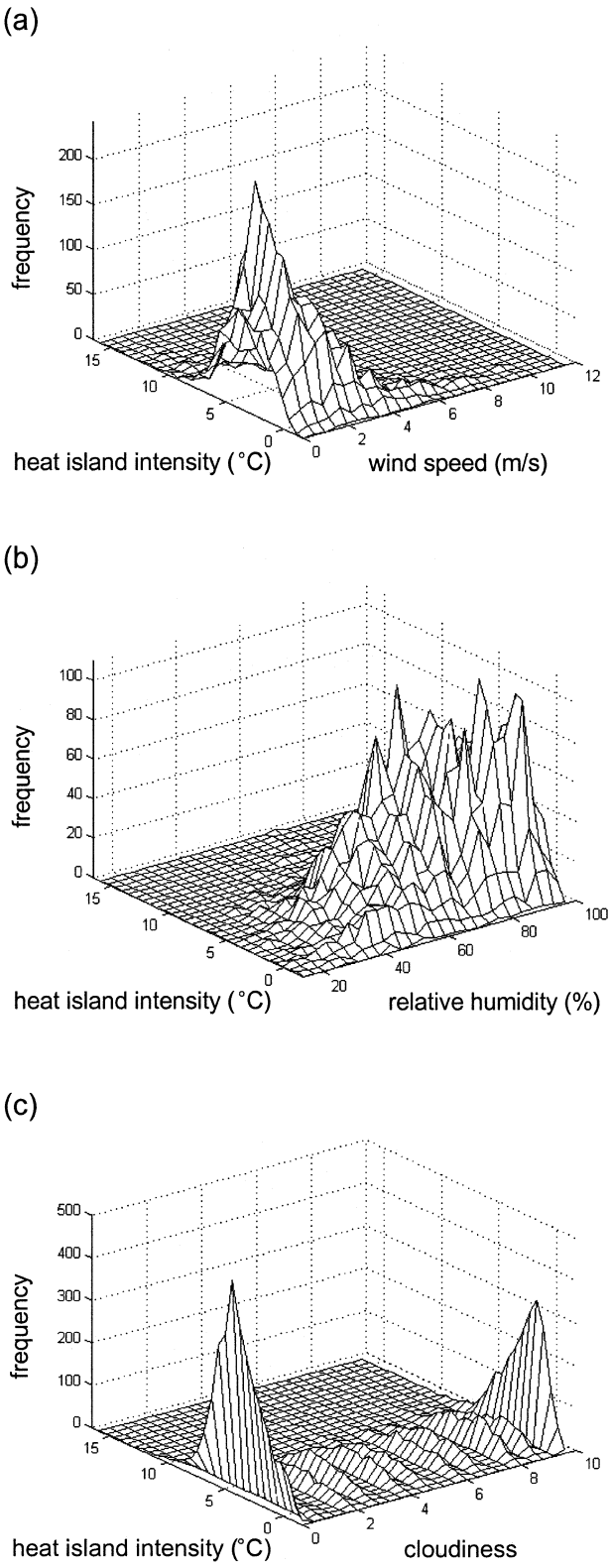

FIG. 6. The frequency distribution of the maximum temperature deviation between Seoul and Yangpyong observatories as a function of (a) wind speed, (b) relative humidity, and (c) cloudiness.

TABLE 1. Normalized regression coefficients of the four meteorological predictors (PER, maximum UHI intensity for the previous day; WS, wind speed; CL, cloudiness; RH, relative humidity). All regression coefficients are statistically significant at the 95% confidence level except for that with superscript (*). Here, r^2 is the percent of total variance explained by the multiple linear regression model, and n is the sample size.

	All	Daytime	Nighttime	Spring	Summer	Autumn	Winter
PER	0.52	0.43	0.52	0.31	0.37	0.42	0.53
WS	−0.24	−0.27	−0.23	−0.34	−0.17	−0.26	−0.27
CL	−0.21	−0.18	−0.21	−0.24	−0.24	−0.28	−0.13
RH	−0.12	−0.04	−0.16	−0.14	−0.28	−0.14	−0.00*
r^2 (%)	46.1	32.4	51.9	32.5	43.1	41.6	39.7
n	8765	8765	8765	2208	2207	2184	2166

UHI intensity and relative humidity, but it will be shown in the next section that they are negatively correlated.

The frequency distribution of the maximum UHI intensity as a function of cloudiness is shown in Fig. 6c. The number of days with cloudiness 0 at the time of the maximum UHI intensity in Seoul is 3480 (40% of the total data). The number of days with cloudiness 10 at the time of the maximum UHI intensity is 2100 (24% of the total data). This occurrence frequency seems to be high, although the value of cloudiness is assigned as 10 when it is rainy or snowy or foggy. A plausible reason might be that the observers were inclined to assign 10 for the cloudiness when the sky is almost covered with clouds during the nighttime. The most prominent occurrence of the maximum UHI intensity has a peak at 4.5°C when the cloudiness is 0. A secondary peak is observed at 1.7°C when the cloudiness is 10. Well-defined UHI phenomena are observed even when the sky is completely covered by clouds or precipitation or fog exists, but the maximum UHI intensities are usually much weaker than those when there are no clouds.

b. Regression analysis

In the regression analysis, the dependent variable is the maximum UHI intensity and the independent variables (predictors) are the four meteorological elements. Before the multiple linear regression analysis is performed, each of the dependent and independent variables is subtracted from the mean and then divided by the standard deviation. With this normalization, a comparison of regression coefficients for different variables is possible.

Table 1 shows normalized regression coefficients for the four meteorological predictors and the percent of total variance explained by the multiple linear regression model. The values in the second column of Table 1 are normalized regression coefficients calculated using unstratified data. The values in the third and fourth columns are normalized regression coefficients calculated using partitioned data with daytime and nighttime. The values in the fifth to eighth columns are normalized regression coefficients calculated using stratified data with season.

The case in which data are unstratified (second column of Table 1) is examined first. The most important predictor among the four variables is the maximum UHI intensity for the previous day (PER). The maximum UHI intensity tends to be strong if the maximum UHI intensity for the previous day was strong. The normalized regression coefficient of PER is 0.52. PER is largely dependent upon the duration of certain types of weather. The second most important predictor is the wind speed (WS). As expected, WS is negatively correlated with the maximum UHI intensity, meaning that the latter is weakened as the wind speed increases. When the wind speed increases, enhanced temperature advection and turbulent activity reduce thermal contrast between the urban and rural areas.

The third most important predictor is the cloudiness (CL). The correlation between CL and the maximum UHI intensity is negative. When the sky is cloudy, clouds absorb longwave radiation from the surface and emit it back, so the variation in diurnal temperature is reduced (Oke 1987), resulting in a negative correlation. The least important predictor is the relative humidity (RH). The RH is negatively correlated with the maximum UHI intensity. When evaporation from the urban surface takes place, the surface air temperature decreases because of evaporative cooling, and the relative humidity increases because of an increase in water vapor pressure and a decrease in saturation water vapor pressure. Hence, the maximum UHI intensity tends to decrease as the relative humidity increases.

The total variance explained by the regression model is 46.1%. This small proportion of the total variance suggests that other relevant predictors, including those related to synoptic weather and anthropogenic heat, need to be included to increase the variance explained. Further research is needed to investigate other relevant predictors.

Another regression analysis is performed in which the relative humidity predictor is replaced by the water vapor pressure predictor (WVP) while the other three predictors (PER, WS, CL) are kept the same. The regression coefficients of PER, WS, CL, and WVP are 0.50, −0.24, −0.22, and −0.13; the total variance explained by the regression model is 46.4%. These values are very similar to those in the second column of Table 1. This similarity indicates that the water vapor pressure predictor can be used equally well as the relative hu-

midity predictor in a study of the maximum UHI intensity in Seoul.

The data are partitioned into daytime and nighttime datasets to examine the day–night dependency of the four predictors in relation to the maximum UHI intensity. In this partition, the daytime (nighttime) maximum UHI intensity is the maximum temperature difference between Seoul and Yangpyong observatories during daytime (nighttime). As shown in Table 1, the order of the magnitude of the regression coefficients for the four predictors and the signs of the regression coefficients for the daytime and nighttime datasets are the same as those for the total dataset. The magnitude of each regression coefficient of PER, CL, and RH is larger in the nighttime than in the daytime. On the other hand, the magnitude of the regression coefficient of WS is smaller in the nighttime than in the daytime. The total variance explained in the nighttime (51.9%) is larger than that in the daytime (32.4%). This result is consistent with the Sundborg's (1950) result.

To examine seasonal dependency, the total data are stratified with season and the regression analysis is again performed. Results are given in Table 1. The sign of each regression coefficient for seasonally stratified datasets is the same as that for the total dataset, but the order of the magnitude of the regression coefficient is different, depending on season. In spring, the most important predictor is wind speed. In summer, which has much larger precipitation amounts than do other seasons, the relative humidity is the second most important predictor. In autumn, the cloudiness is the second most important predictor, with the magnitude of its regression coefficient being slightly larger than that of the regression coefficient of the wind speed. In winter, the persistence predictor is dominant over the other three predictors relative to other seasons. The regression coefficient of the relative humidity in winter is not statistically significant at the 95% confidence level. The total variance is largest in summer (43.1%) and smallest in spring (32.5%).

c. Neural network model

Next, experiments for predicting the maximum UHI intensity in Seoul are conducted using a neural network model, and its performance is compared with that of a multiple linear regression model. In this study, a back-propagation neural network is employed, which is composed of a layer of input units, a layer (or layers) of hidden units, and a layer of output units. The back-propagation neural network repeatedly adjusts connection weights between hidden units and output units and between input units and hidden units in a way that the error between desired output and actual output is minimized (Rumelhart et al. 1986). The core algorithm of the standard back-propagation neural network in the Stuttgart Neural Network Simulator (SNNS; Zell et al. 1998) is adopted for this study and can be written as

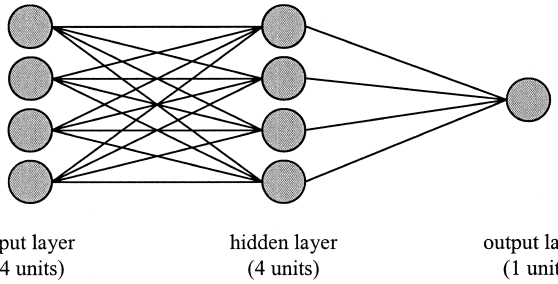

FIG. 7. The structure of a three-layer neural network constructed in this study. The input layer, hidden layer, and output layer have 4 units, 4 units, and 1 unit, respectively.

$$\Delta w_{ij} = \eta \delta_j o_i, \tag{1}$$

where

$$\delta_j = \begin{cases} f_j'(x_j)(d_j - o_j) & \text{if unit } j \text{ is an output unit,} \\ f_j'(x_j) \sum_k \delta_k w_{jk} & \text{if unit } j \text{ is a hidden unit.} \end{cases} \tag{2}$$

Here, i is the index of a predecessor to the current unit j with link w_{ij} from i to j, j is the index of the current unit, and k is the index of a successor to the current unit j with link w_{jk} from j to k. Also, Δw_{ij} are the changes in connection weights, δ_j is the error of unit j, d_j is the desired output of unit j, and o_i is the output of the preceding unit i. The learning rate, η in (1), is related to the speed of error convergence. The x_j in (2) is a sum of connection weights multiplied by outputs. The activation function f in (2) with its derivative f' is introduced to take nonlinearity into account in the neural network and is usually given in a sigmoid function that takes values between 0 and 1. Data are partitioned into the training (or learning) dataset, validation dataset, and test (or prediction) dataset to generalize the neural network best. The learning process is usually repeated until the error for the validation dataset becomes minimum.

The structure of a three-layer neural network constructed in this study is shown in Fig. 7. The input layer has four units (PER, WS, CL, and RH predictors), the hidden layer has four units, and the output layer has one unit (maximum UHI predictand). This neural network structure was found to give a minimum prediction error among tested cases with different hidden layers and different units in a hidden layer. The 24-yr dataset is split into the training (80% of the total data), validation (10%), and test datasets (10%). The learning rate is specified as 0.05. The number of epochs is between 2000 and 4000 for this dataset. Before neural computation, the predictand is properly normalized to have values between 0 and 1 and each of the predictors is also normalized to have values between -1 and 1 (Baik and Hwang 1998; Baik and Paek 2000). For further details of the neural network, see Rumelhart et al. (1986) and Zell et al. (1998), and for an application of the neural network, see Baik and Paek (2000).

To examine the performance of the above-mentioned

TABLE 2. Average UHI intensity (°C) in Seoul (upper values, 10% test data; lower values in parentheses, total data) and the average prediction errors of the maximum UHI intensity from the multiple linear regression model and the neural network model. Here, *N* is the number of prediction–experiment cases.

	All	Daytime	Nighttime	Spring	Summer	Autumn	Winter
UHI intensity	3.41	2.26	3.25	3.24	2.00	4.35	4.33
	(3.39)	(2.22)	(3.23)	(3.17)	(2.02)	(4.28)	(4.22)
Regression prediction error	1.26	1.32	1.22	1.18	0.88	1.12	1.53
Neural prediction error	1.18	1.24	1.18	1.17	0.87	1.07	1.43
N	876	876	876	220	220	218	216

neural network model against a traditional statistical model in predicting the maximum UHI intensity in Seoul, a multiple linear regression model is constructed. Each of the dependent and independent variables is normalized, as described earlier. The same 80% dataset (learning dataset) in the neural network model is utilized to obtain a multiple linear regression equation, and the same 10% dataset (test dataset) is utilized to do prediction experiments.

Table 2 shows the average prediction errors from the multiple linear regression model and the neural network model, together with the average maximum UHI intensity. Here, the average prediction error represents the average of absolute prediction errors of the maximum UHI intensity for the prediction (test) dataset. The average maximum UHI intensities for the test dataset are very similar to those for the total dataset. For the unstratified test data, the average maximum UHI intensity is 3.41°C and the average prediction errors from the regression model and the neural network model are 1.26° and 1.18°C, respectively. Therefore, the neural network model improves upon the regression model by 6.3%. When the data are partitioned into the daytime and nighttime datasets, it is revealed, as expected, that the nighttime maximum UHI intensity is stronger than the daytime one. The prediction error from the neural network model is smaller than that from the regression model for both stratified datasets. The improvement of the neural network model upon the regression model is higher in the daytime (6.1%) than in the nighttime (3.3%). When the data are stratified with season, it is revealed that the maximum UHI intensity is highest in autumn and weakest in summer. The neural network model improves upon the regression model in all seasons, ranging from 0.8% in spring to 6.5% in winter. The reason for the improvement of the neural network model upon the multiple linear regression model in predicting the maximum UHI intensity in Seoul is that the neural network has an internal ability to take complex nonlinear interactions into account. This ability is achieved by including the nonlinear activation function in the neural network.

Multiple nonlinear regression analysis is undertaken to evaluate the performance of multiple nonlinear regression model relative to that of the multiple linear regression model or neural network model. For this evaluation, two multiple nonlinear regression models (power and quadratic regression models) are developed. The total variance explained by the power regression model ($PER^aWS^bCL^cRH^d$, where *a, b, c,* and *d* are the determined exponents) is 38.1% for the total data. This percentage is smaller than the total variance of the multiple linear regression model (46.1%). This result is qualitatively consistent with that of Morris et al. (2001), who examined the influences of wind and cloud on the nocturnal urban heat island of Melbourne, Australia. The average prediction error of the maximum UHI intensity in Seoul is 1.34°C for the test data. This error is larger than that from the multiple linear regression model (1.26°C). In the development of a quadratic regression model, the quadratic combinations of the four predictors are considered, together with the four linear predictors (PER, WS, CL, RH). Among 10 potential quadratic predictors, only 2 quadratic predictors are retained after the removal of predictors with large variance inflation factors. The final quadratic regression model includes the 4 linear predictors and 2 quadratic predictors. The total variance explained by the quadratic regression model is 46.3% for the total data. The average prediction error from the quadratic regression model (1.23°C) is smaller than that from the multiple linear regression model (1.26°C) but is larger than that from the neural network model (1.18°C).

The above results indicate that a multiple nonlinear regression model can improve upon a multiple linear regression model in the prediction of the maximum UHI intensity if a nonlinear functional relationship between dependent and independent variables is well chosen. The above results also indicate that it might be possible to develop a multiple nonlinear regression model that competes with a neural network model if a best-performed nonlinear functional relationship is chosen.

Sarle (1994) presented the connection between neural networks and statistical models. The back-propagation neural network employed in this study corresponds to the multiple nonlinear regression model. Hence, it might be possible, in principle, to develop a multiple nonlinear regression model that competes with a neural network model. However, in the development of a multiple nonlinear regression model, the task of finding an optimum nonlinear functional relationship between dependent and independent variables is extremely difficult. Moreover, physical interpretations for nonlinear terms are not always possible. Sarle (1994) stated that neural net-

works and statistics are not competing methodologies for data analysis and prediction and that better communication between the two fields would benefit both. For example, as was done in this study, the multiple linear regression method can greatly facilitate the choice of input units for the neural network and some physical interpretations.

4. Summary and conclusions

This study examined the maximum urban heat island intensity (UHI) in Seoul, Korea, using data at two meteorological observatories (an urban site and a rural site) during the period 1973–96. The average maximum UHI intensity was found to be weakest in summer and strong in autumn and winter. The maximum UHI intensity more frequently occurred in the nighttime than in the daytime, decreased with increasing wind speed, and was pronounced for clear skies. Results of the multiple linear regression analysis with four predictors (maximum UHI for the previous day, wind speed, cloudiness, and relative humidity) showed that the previous-day maximum UHI intensity is positively correlated with the maximum UHI intensity, while the wind speed, cloudiness, and relative humidity are negatively correlated with the maximum UHI intensity. The previous-day maximum UHI intensity was the most important predictor, and the relative importance among the predictors varied depending on time of day and season. To predict the maximum UHI intensity in Seoul, a back-propagation neural network model with the four predictors was constructed, and its performance was evaluated relative to that of a multiple linear regression model. The neural network model was proven to improve upon the regression model in predicting the maximum UHI intensity.

In this study, data at the two meteorological observatories with long-term records were utilized to examine the maximum UHI intensity in Seoul. In recent years, many automatic weather stations (AWS) have been installed in the Seoul metropolitan area. These stations are operated by the Korea Meteorological Administration. Using the 1999 AWS data (24 stations in Seoul and 5 stations located on the outskirts of Seoul), Boo and Oh (2000) studied the spatial and temporal variations of the Seoul UHI intensity. Although the number of years for which the AWS data are currently available is very small when compared with the 24-yr period in this study, the accumulating data should provide a better opportunity to study the characteristics of the Seoul UHI phenomenon.

The UHI intensity is strongly influenced by synoptic and mesoscale circulations. Runnalls and Oke (1998) showed that the UHI intensity in Vancouver, Canada, is affected by land–sea breeze circulations. Because of its proximity to the Yellow Sea (between Korea and China), Seoul is under the strong influence of sea breezes, especially in summer. The controls of synoptic and mesoscale circulations on the UHI intensity in Seoul need to be investigated with categorized circulation types.

Acknowledgments. The authors are very grateful to Dr. Marvin Wesely of Argonne National Laboratory and three anonymous reviewers for providing invaluable suggestions on this paper, which led to substantial improvement of an original manuscript. This research was supported by the Climate Environment System Research Center sponsored by the SRC Program of the Korea Science and Engineering Foundation. This research was also supported by the Brain Korea 21 Project.

REFERENCES

Ackerman, B., 1985: Temporal march of the Chicago heat island. *J. Climate Appl. Meteor.*, **24,** 547–554.

Baik, J.-J., and H.-Y. Chun, 1997: A dynamical model for urban heat islands. *Bound.-Layer Meteor.,* **83,** 463–477.

——, and H.-S. Hwang, 1998: Tropical cyclone intensity prediction using regression method and neural network. *J. Meteor. Soc. Japan,* **76,** 711–717.

——, and J.-S. Paek, 2000: A neural network model for predicting typhoon intensity. *J. Meteor. Soc. Japan,* **78,** 857–869.

——, Y.-H. Kim, and H.-Y. Chun, 2001: Dry and moist convection forced by an urban heat island. *J. Appl. Meteor.*, **40,** 1462–1475.

Boo, K.-O., and S.-N. Oh, 2000: Characteristics of spatial and temporal distribution of air temperature in Seoul, 1999 (in Korean). *J. Korean Meteor. Soc.*, **36,** 499–506.

Changnon, S. A., Jr., Ed., 1981: *METROMEX: A Review and Summary. Meteor. Monogr.*, No. 40, Amer. Meteor. Soc., 181 pp.

Cotton, W. R., and R. A. Pielke, 1995: *Human Impacts on Weather and Climate.* Cambridge University Press, 288 pp.

Duckworth, F. S., and J. S. Sandberg, 1954: The effect of cities upon horizontal and vertical temperature gradients. *Bull. Amer. Meteor. Soc.*, **35,** 198–207.

Hsieh, W. W., and B. Tang, 1998: Applying neural network models to prediction and data analysis in meteorology and oceanography. *Bull. Amer. Meteor. Soc.*, **79,** 1855–1870.

Jauregui, E., L. Godinez, and F. Cruz, 1992: Aspects of heat-island development in Guadalajara, Mexico. *Atmos. Environ.,* **26B,** 391–396.

Karaca, M., M. Tayanc, and H. Toros, 1995: Effects of urbanization on climate of Istanbul and Ankara. *Atmos. Environ.,* **29,** 3411–3421.

Klysik, K., and K. Fortuniak, 1999: Temporal and spatial characteristics of the urban heat island of Lodz, Poland. *Atmos. Environ.*, **33,** 3885–3895.

Lin, Y.-L., and R. B. Smith, 1986: Transient dynamics of airflow near a local heat source. *J. Atmos. Sci.,* **43,** 40–49.

Lowry, W. P., 1998: Urban effects on precipitation amount. *Prog. Phys. Geogr.*, **22,** 477–520.

Montavez, J. P., A. Rodriguez, and J. I. Jimenez, 2000: A study of the urban heat island of Granada. *Int. J. Climatol.*, **20,** 899–911.

Morris, C. J. G., I. Simmonds, and N. Plummer, 2001: Quantification of the influences of wind and cloud on the nocturnal urban heat island of a large city. *J. Appl. Meteor.*, **40,** 169–182.

Oke, T. R., 1987: *Boundary Layer Climates.* 2d ed. Routledge, 435 pp.

——, G. T. Johnson, D. G. Steyn, and I. D. Watson, 1991: Simulation of surface urban heat islands under 'ideal' conditions at night. Part 2: Diagnosis and causation. *Bound.-Layer Meteor.,* **56,** 339–358.

Rumelhart, D. E., G. E. Hinton, and R. J. Williams, 1986: Learning representations by back-propagating errors. *Nature,* **323,** 533–536.

Runnalls, K. E., and T. R. Oke, 1998: The urban heat island of Vancouver, BC. Preprints, *Second Urban Environment Symp.,* Albuquerque, NM, Amer. Meteor. Soc., 84–87.

Santamouris, M., G. Mihalakakou, N. Papanikolaou, and D. N. Asimakopoulos, 1999: A neural network approach for modeling the heat island phenomenon in urban areas during the summer period. *Geophys. Res. Lett.*, **26,** 337–340.

Sarle, W. S., 1994: Neural networks and statistical models. *Proc. 19th Annual SAS Users Group Int. Conf.*, Dallas, TX, SAS Institute, 1538–1550. [Available online at http://www.sas.com.]

Sundborg, A., 1950: Local climatological studies of the temperature conditions in an urban area. *Tellus*, **2,** 222–232.

Yague, C., E. Zurita, and A. Martinez, 1991: Statistical analysis of the Madrid urban heat island. *Atmos. Environ.*, **25B,** 327–332.

Zell, A., and Coauthors, 1998: SNNS, Version 4.2, user manual. University of Stuttgart, 345 pp. [Available online at ftp://ftp.informatik.uni-tuebingen.de/pub/SNNS.]